

## Mechanical Properties of Epoxy Composites with Low Content of Diamond Particles

Sobia A. Rakha,<sup>1</sup> Ramsha R. Khan,<sup>1</sup> Aqeel A. Khurram,<sup>1</sup> A. Fayyaz,<sup>1</sup> M. Zakauallah,<sup>2</sup> Arshad Munir<sup>1</sup>

<sup>1</sup>Department of Materials Science, Centre of Excellence for Science and Advanced Technology, Islamabad, 45320, I. R. Pakistan

<sup>2</sup>Department of Physics, Quaid-i-Azam University, Islamabad, 45320, I. R. Pakistan

Correspondence to: A. Munir (E-mail: arshad.dr@gmail.com)

**ABSTRACT:** Diamond-epoxy composites reinforced with low content of submicron diamond powder 0.1, 0.4, 0.7, and 1.0 wt % were synthesized. As received diamond powder was acid treated to purify and functionalize diamond particles. Fourier Transform Infrared Spectroscopy was utilized to study the moieties attached to the diamond particles. The trace elemental analysis of impurities in diamond powder before and after acid treatment was performed using ion beam techniques. The mechanical properties of the epoxy matrix were enhanced with the addition of purified and functionalized diamond powder. The Dynamical mechanical analysis results revealed that storage modulus of the prepared composites has been increased by  $\sim 100\%$  with diamond loading of 0.7 wt %. The Vickers's hardness of the diamond-epoxy composite was  $\sim 39\%$  higher than that of pure epoxy for the loading of 1.0 wt % diamond powder. Mechanisms responsible for the enhancement of the mechanical properties are discussed. © 2012 Wiley Periodicals, Inc. *J. Appl. Polym. Sci.* 000: 000–000, 2012

**KEYWORDS:** dispersions; fillers; spectroscopy; hardness; mechanical properties

Received 17 February 2012; accepted 4 May 2012; published online

**DOI:** 10.1002/app.38029

### INTRODUCTION

Carbon-related materials with small particle size are promising candidates for a variety of applications in electronics, biology, and composite materials. Diamond being  $sp^3$  form of carbon is potentially applicable candidate for composite formation due to its superior hardness and thermal conductivity. The wide band gap of the diamond ( $\sim 5$  eV) renders it highly absorptive toward UV light, but transparent in the visible and IR range.<sup>1,2</sup> Diamond powder (DP), being biocompatible<sup>3</sup> can be used as a filler of a polymer matrix in many applications. Diamond containing fibers could be used in smart and UV-protecting clothing, for biomedical applications such as wound dressings,<sup>4</sup> sensing,<sup>5</sup> and drug delivery systems.<sup>6,7</sup> However, careful characterization and purification of DP is required to ensure quality<sup>8</sup> and achieve a better control of the surface chemistry<sup>9,10</sup> and particle size,<sup>11</sup> prior to its use in any matrix for different applications. Recent studies have shown that an air oxidation process dramatically increases the purity of DP,<sup>9</sup> allowing to control the ratio of  $sp^2$  to  $sp^3$  carbon and surface chemistry of DP.<sup>12</sup>

Low density of polymers and less expensive methods of synthesis of the polymer-based matrix composites tend to be far superior, making it highly advantageous to use them in light weight structures in aerospace and transportation industries. Several

recent studies focused on the incorporation of DP into thermoplastic polymers.<sup>13,14</sup> However, the DP composites with thermosetting polymers are far less studied.<sup>15–20</sup> Epoxy resins are among the most versatile thermoset polymers for industrial applications.

The epoxies can be used without solvent and therefore without volatile by product during curing and thus low volume shrinkage. The lack of solvents makes epoxies usable with almost every type of core material. The epoxy resins have generally quite good mechanical properties. However, as the majority of polymeric materials, the epoxy has poor thermal conductivity, which is a limiting factor in many technological areas, such as electronic and aerospace.<sup>21</sup> The thermal and mechanical properties of epoxy resin can be improved by adding fillers such as diamond; diamond, known for its extremely high  $E$  (elastic modulus) value, above 1000 GPa is expected to increase the  $E$  of the composite remarkably. The performance of diamond as a filler in epoxy matrices depends on the proper association of the hard diamond particles and the soft polymeric matrix. The nanofiller concentration at the dilute limit has been reported to enhance the mechanical properties of diamond-epoxy composites<sup>15</sup> whereas the higher concentrations of diamond particles lead to agglomeration of the powders.<sup>22</sup> Monteiro et al.<sup>15</sup> studied the mechanical characteristics of diamond reinforced epoxy

composites using high content of diamond. Their results showed that the dynamic mechanical parameters are improved with the amount of diamond particles and markedly affected by modifications in the epoxy matrix. However, the quasi-static mechanical properties were decreased with the amount of diamond. This behavior was attributed to the development of a weak diamond/epoxy interface and corroborated by the analysis of the fracture surfaces as well as the variation of the dynamic mechanical parameters for the investigated conditions.

Here we presented the results which highlight the peculiarities of the DP when used as a mechanical reinforcement in polymer composites. We focus on composites with low loading of sub-micron diamond crystallites (0.1, 0.4, 0.7, and 1.0 wt %) since it provides a case for good dispersion of the particles in the matrix and the properties of the epoxy matrix preserved with moderate enhancement in mechanical properties.

## EXPERIMENTAL

### Materials

The DP was supplied by Shanghai flash hardware abrasive factory. As-received DP was characterized using scanning electron microscope (SEM), X-ray diffractometer (XRD), and Fourier Transform Infrared (FTIR) spectroscopy for morphology, structure and bonding characterizations. The impurities in DP mainly consist of nondiamond (amorphous and graphitic) carbon and traces of metals embedded into the amorphous carbon shells.<sup>12</sup> Before incorporation into the polymer matrix, DP was purified by air oxidation (2 h at 430°C) to remove nondiamond carbon and further refluxed in concentrated H<sub>2</sub>SO<sub>4</sub>/HNO<sub>3</sub> at 300°C for 24 h to remove metals and metal oxides. Acid reflux was performed using 100 mg of DP in 9 : 1 of H<sub>2</sub>SO<sub>4</sub> and HNO<sub>3</sub>.<sup>23</sup> The acid-refluxed DP was centrifuged with distilled water until reaching neutral pH. The purpose of acid treatment is to create surface carboxyl and hydroxyl groups, which can interact with the polymer matrix at molecular level. The refluxed DP powder was characterized using FTIR spectroscopy after drying. Acid-treated DP was dispersed ultrasonically in epoxy matrix (Epon 828; diglycidyl ether of bisphenol A) using Branson 1510 ultra-sonicator. The stoichiometry of Epon 828 is well known and described elsewhere.<sup>24</sup> Composites were prepared with up to 1.0 wt % loading of diamond particles in the liquid epoxy matrix. After 2 h of sonication, the composite was degassed for 30 min to remove air bubbles. The composites were then cured with a triethylene tetra-amine (TETA) hardener by thoroughly mixing and degassing using same high power ultrasonic system. The composites were cast into respective dies and were left for overnight at room temperature. Further curing was done under heating cycle at 150°C for 3 h in an oven.

### Measurements

The XRD patterns and FTIR spectra of as received and acid-treated DP were obtained using CuK $\alpha$  source ( $\lambda = 0.1541$  nm), D/max-2200 X-ray Diffractometer and Thermo Electron Corporation IR 200 FTIR spectrometer respectively. The ion beam analyses (IBA) of both as-received and acid refluxed DP were performed using 5UDH Pelletron Tandem accelerator at Experimental Physics Lab, NCP, Islamabad. The rectangular  $40 \times 8 \times 1$  mm<sup>3</sup> specimens were prepared for dynamical mechanical anal-

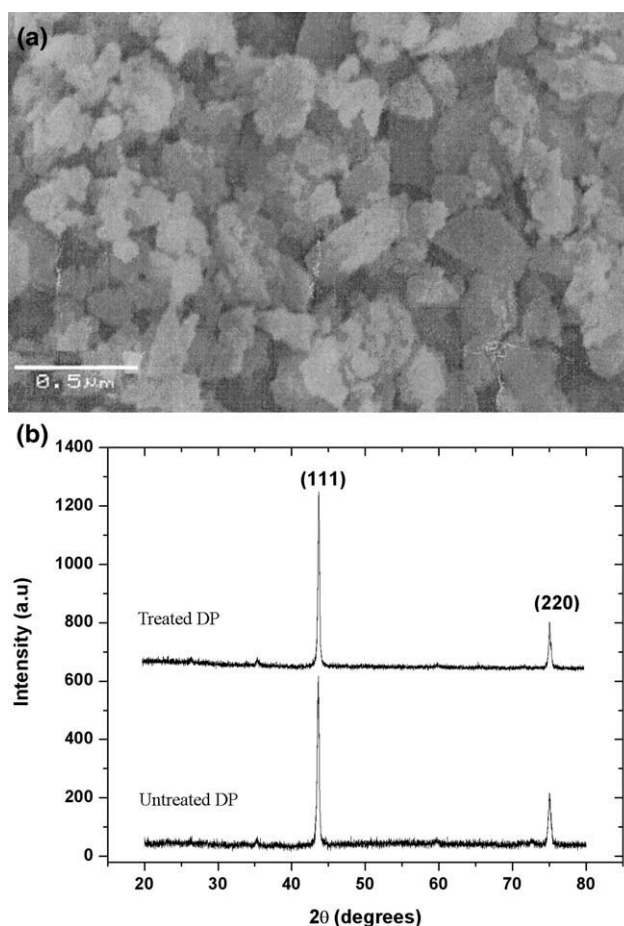


**Figure 1.** (a) SEM image of as received DP, (b) XRD patterns of untreated and treated DP.

ysis (DMA), using DMA-7 Perkin Elmer equipment operating at 0.1 Hz. The storage modulus ( $E'$ ), loss modulus ( $E''$ ), and delta tangent ( $\tan \delta$ ), curves were recorded in the DMA tests. Microhardness measurements are performed using Wilson Instrument 401 MVA Vickers microhardness tester equipped with a 136° diamond indenter. An imposed load of 490 mN on the samples was utilized for a dwell time of 15 s. The morphology of diamond-epoxy composites was studied using a SEM (JED 2300).

## RESULTS AND DISCUSSION

### Characterizations

The SEM image of submicron diamond particles is shown in Figure 1(a). The average size of the diamond particles is in the range of 500 nm. There are also few particles present in the powder and shown in the image with size smaller than 500 nm. The XRD patterns of as-received and acid-treated DP is shown in Figure 1(b). Two diffraction peaks at  $2\theta \sim 43.8^\circ$  (111) and  $75.2^\circ$  (220) corresponds to the cubic planes of diamond. There is no obvious background from amorphous carbon indicating the high quality of the DP before and after acid treatment. The diffraction spectra of as-received and acid-treated DP are identical; indicating that no change in crystallite size or quality is arose from this process.

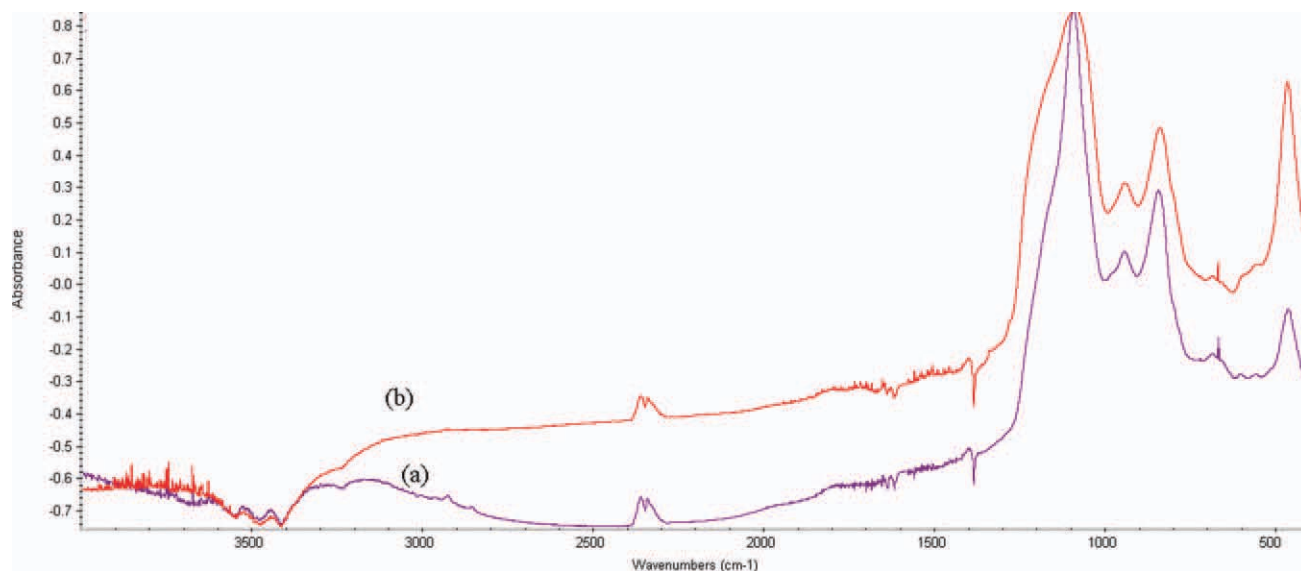


**Figure 2.** FTIR spectra of (a) untreated and (b) treated DP. [Color figure can be viewed in the online issue, which is available at [wileyonlinelibrary.com](http://www.wileyonlinelibrary.com).]

FTIR spectroscopy has been used to detect the surface functional groups of DP. FTIR spectra of both as received (untreated) and acid-treated DPs are shown in Figure 2. Starting with the low wave numbers, the intensity of the band around  $470\text{ cm}^{-1}$  increased and the bands around  $840$  and  $1000\text{ cm}^{-1}$  are sharp in acid-treated DP in comparison to untreated DP. The band around  $840\text{ cm}^{-1}$  is attributable to aromatic rings. The band starting from  $1000\text{ cm}^{-1}$  with maxima at  $1110\text{ cm}^{-1}$  is due to the superposition of bands associated with  $\equiv\text{C}-\text{O}-\text{C}\equiv$  group.<sup>25</sup> The intensity of this band increased after acid treatment. The features between  $1600$  and  $1700\text{ cm}^{-1}$  are mostly related to water and OH bending. The  $1620\text{ cm}^{-1}$  band is associated with an OH bending mode. A small peak around  $1700\text{ cm}^{-1}$  in the acid-treated DP is due to the presence of carbonyl groups on the treated powder surface.<sup>26</sup>

Figure 3(a, b) shows elemental analysis using Rutherford Backscattering Spectroscopy (RBS), an important IBA technique. The RBS spectra were recorded using  $4.501\text{ MeV}$  beam of  $\text{He}^{2+}$  ions focused to a diameter of  $2\text{ mm}$  by a high-precision system of quadrupole magnetic lenses. Backscattered ions were collected on a silicon surface barrier detector at an angle of  $170^\circ$  as measured with respect to the incident direction of the beam. The spectra shown here were recorded with  $\text{He}^{2+}$  integrated charge of  $20\text{ }\mu\text{C}$ . The setup chamber was maintained at a background vacuum of approximately  $10^{-6}$  Torr. Noncarbon impurities (Fe, Cr, Ni, Al, Si, Ca, etc.) are usually present in the commercially produced DP.<sup>12</sup> The detected elements are Re, Bi, C, and O in untreated [Figure 3(a)] and treated [Figure 3(b)] samples. The spectrum after acid treatment shows increased concentration of carbon from  $78.5$  to  $85.5\%$  and oxygen from  $8.6$  to  $19.9\%$  in the sample. The elements Bi and Re have been reduced from  $0.3$  to  $0.1\%$  and from  $1.2$  to  $0.2\%$ , respectively. SIMNRA simulation code was used to obtain quantitative information from the spectra and results are listed in Table I. The trace elemental analyses of heavy atoms were carried out using Proton Induced

X-ray Emission (PIXE) technique. PIXE spectra for the samples before and after acid treatment are shown in Figure 3(c). The spectra were recorded using  $1.275\text{ MeV}$  of proton beam. Ion beam induced characteristics x-rays were collected using a silicon lithium detector at an angle of  $45^\circ$  as measured with respect to the incident direction of the beam. The PIXE spectra shown here were recorded with  $\text{H}^+$  integrated charge of  $40\text{ }\mu\text{C}$ . It is clear from the relative comparison of the two spectra that the content of noncarbon impurities in the treated DP has been considerably reduced.

### Mechanical Properties

Figure 4 shows the Vickers's hardness with diamond incorporation in epoxy matrix at an imposed load of  $490\text{ mN}$ . Five measurements were conducted at different locations to estimate the average values of micro-hardness for each load. Approximately  $5\%$  variations in hardness values are observed. The Vickers's hardness was increased after the increase of diamond content to  $1.0\text{ wt } \%$ . The obtained Vickers hardness values are ( $10\text{ HV}$ )  $98.7\text{ MPa}$  for neat epoxy and ( $13.8\text{ HV}$ )  $136.3\text{ MPa}$  for the  $1.0\text{ wt } \%$  DP sample. The Vickers's hardness of  $1.0\text{ wt } \%$  diamond-epoxy composite is  $39\%$  higher than that of the pure epoxy.

The reinforcement effect of the DP in the wide range of temperature (from  $25$  to  $160^\circ\text{C}$ ) was revealed by DMA. Figure 5 illustrates the storage modulus ( $E'$ ), loss modulus ( $E''$ ) and  $\tan\delta$ , as registered, DMA curves of the blank and diamond-epoxy composites with different percentages of loading of diamond particles in epoxy matrix. Storage modulus is associated with the stored energy, which is released upon stress withdrawal; Figure 5(a) shows  $E'$  as a function of temperature. The addition of DP to the epoxy network increased the  $E'$  value from  $2787\text{ MPa}$  (for neat epoxy) to  $5746\text{ MPa}$ ,  $\sim 100\%$  increase in the value of storage modulus (for DP content of  $0.7\text{ wt } \%$ ). However, the increase in the DP concentration to  $1.0\text{ wt } \%$  leads to a decrease in the modulus to  $3529\text{ MPa}$  but still higher than neat epoxy.

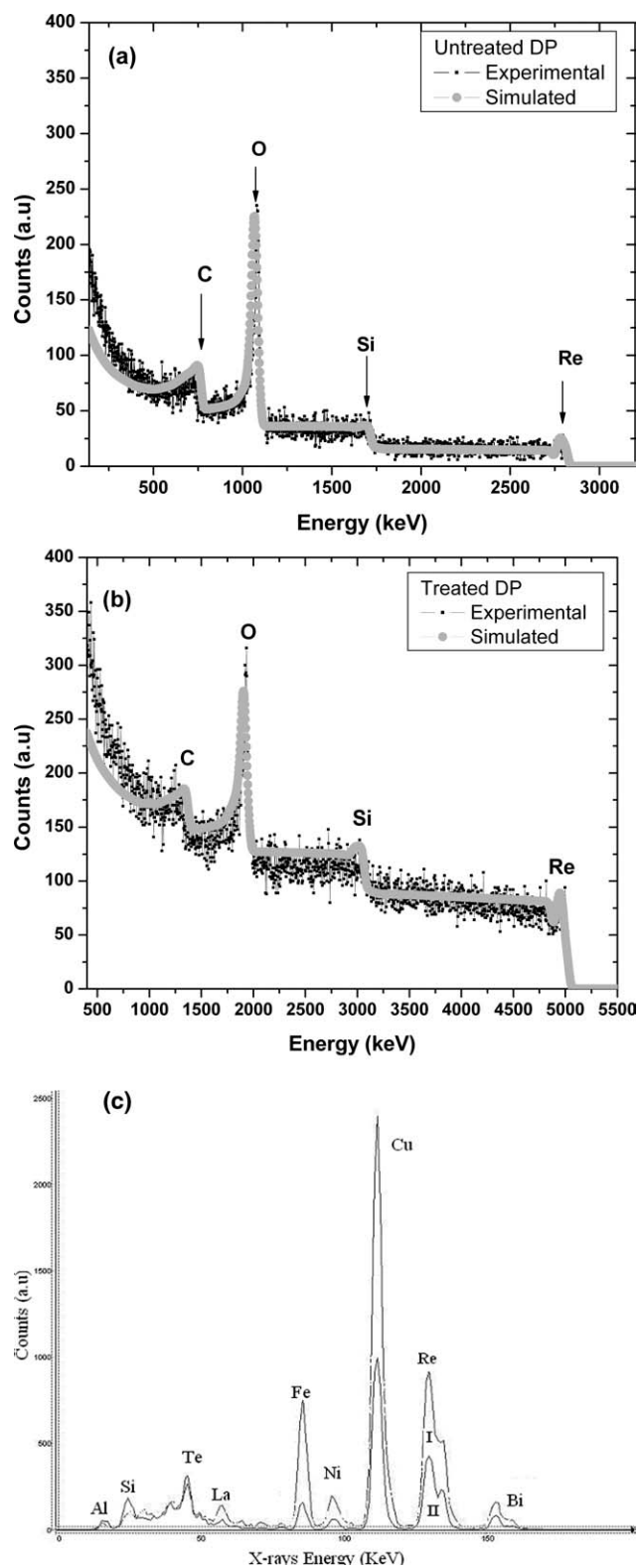


**Figure 3.** RBS for (a) untreated and (b) treated DP; (c) PIXE spectra of (solid line indicated by curve I) untreated and treated (dotted line indicated by curve II) DP.

For the  $\tan \delta$ , the main dispersion, so-called  $\alpha_a$ , around  $127^\circ\text{C}$  is assigned as the glass transition ( $T_g$ ) of the epoxy matrix. The peak of this  $\alpha_a$  dispersion of the diamond-epoxy composites

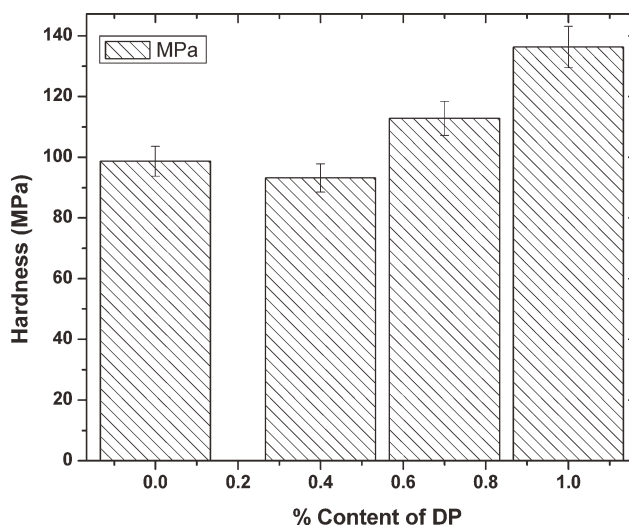
**Table I.** Elemental Analysis for Untreated and Treated DP

Elements	Untreated	Treated
Bi	0.28%	0.13%
C	78.54%	83.42%
O	8.46%	10.54%
Si	11.50%	5.78%
Re	1.22%	0.13%

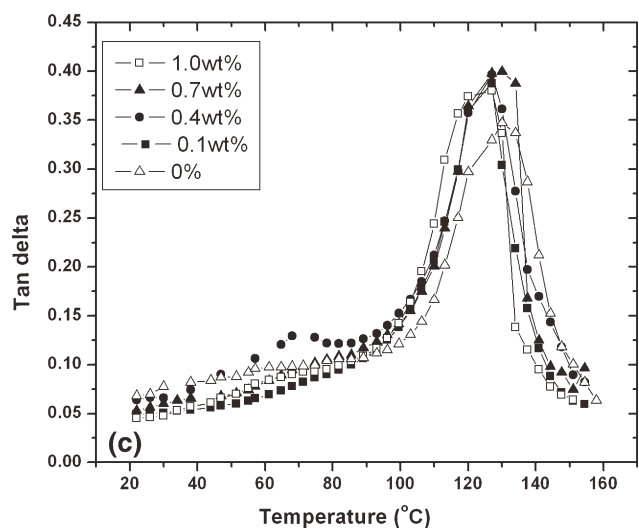
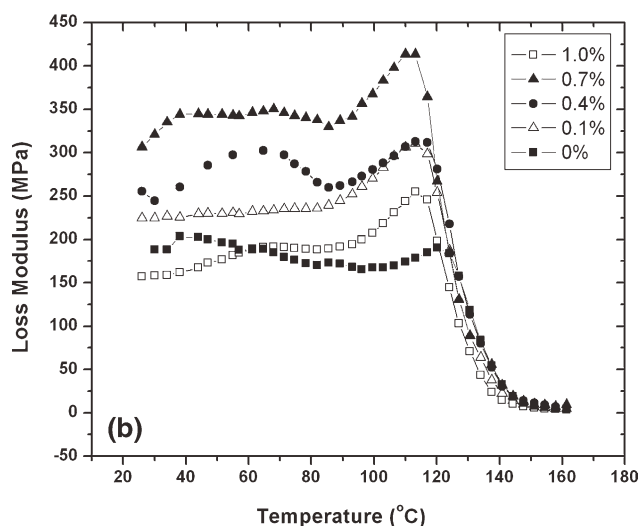
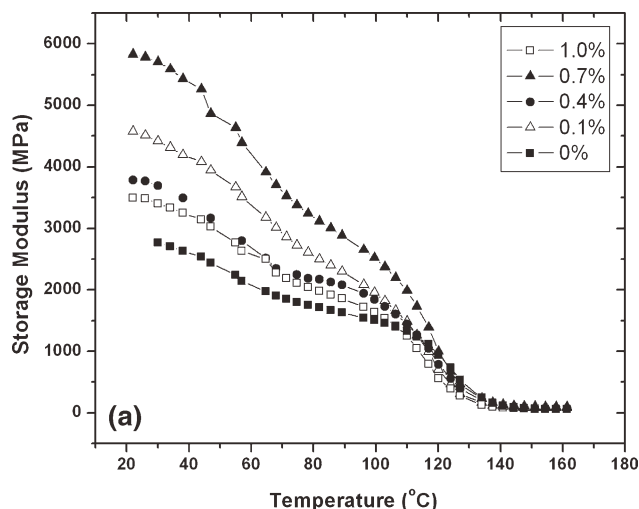
with 0.7 wt % DP loading shifted to a higher temperature ( $130^\circ\text{C}$ ). This is due to reason that the diamond particles restrict the segmental motion of polymer chains in the composite that results in a high value of  $T_g$ .<sup>27–30</sup> Being a hard and stiff phase, the diamond is impairing the matrix mobility by efficiently restricting the movements of the epoxy molecular network. Increasing the DP concentration up to 1.0 wt %, resulted in a decrease of the thermo-mechanical properties, which may be attributed to the conglomeration of DP in the matrix. The DMA results of diamond-epoxy composites with different weight percentages are listed in Table II.

Figure 6 shows the comparison in storage and loss modulus of treated and untreated DP in epoxy matrix. The data clearly shows the advantage of acid treatment of DPs. The storage [Figure 6(a)] and loss [Figure 6(b)] modulus of treated DPs incorporated in epoxy matrix increases in comparison to untreated DPs in epoxy matrix.

Figure 7 shows the SEM image of the sample with 0.4 wt % DP loading. Figure 7(a) shows the cross sectional view of the sample indicating the diamond particles incorporated in epoxy matrix. The magnified image [Figure 7(b)], shows the fracture marks which is evidence that some interaction exists between the diamond particle and the matrix. SEM image of the sample exhibits a much rougher fracture surface. The increased surface roughness indicates that the path of the crack is distorted by adding DP into the epoxy matrix, making crack propagation



**Figure 4.** Vicker's hardness of diamond-epoxy composites.



**Figure 5.** Temperature dependence of the storage modulus ( $E'$ ) and loss modulus ( $E''$ ) and mechanical  $\tan \delta$  of DP/epoxy composites with DP concentration 0.1, 0.4, 0.7, and 1.0 wt % DP.

more difficult. That is to say, the presence of DP might cause perturbations along the crack front, thus altering the path of the propagating crack.

**Table II.** Storage Modulus ( $E'$ ), Loss Modulus ( $E''$ ), and  $\tan \delta$  of Epoxy and Epoxy-Diamond Composites at 26°C

Sample	Storage modulus $E'$ (MPa)	Loss modulus $E''$ (MPa)	Tan $\delta$ ( $^{\circ}$ C)
Neat Epoxy	2787	189	0.32 (127 $^{\circ}$ C)
Diamond-Epoxy 0.1 wt %	4546	225	0.37 (127 $^{\circ}$ C)
Diamond-Epoxy 0.4 wt %	3810	255	0.38 (128 $^{\circ}$ C)
Diamond-Epoxy 0.7 wt %	5746	308	0.41 (130 $^{\circ}$ C)
Diamond-Epoxy 1.0 wt %	3529	156	0.37 (127 $^{\circ}$ C)

Improvement in properties of epoxy matrix is possible due to homogeneous dispersion of filler in the matrix and through strong interface between matrix and filler. The latter will help to transfer load from matrix to filler more efficiently.

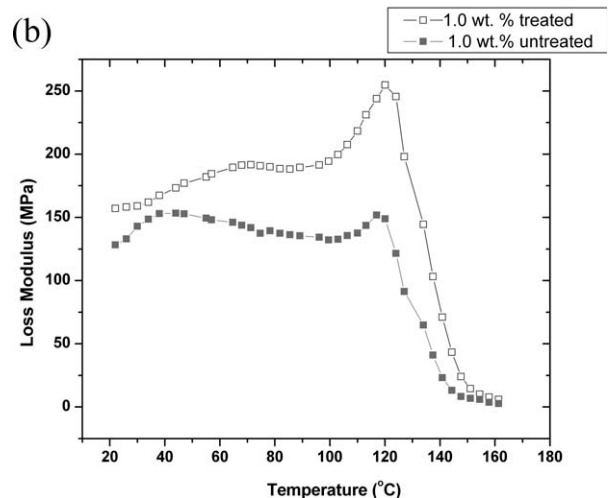
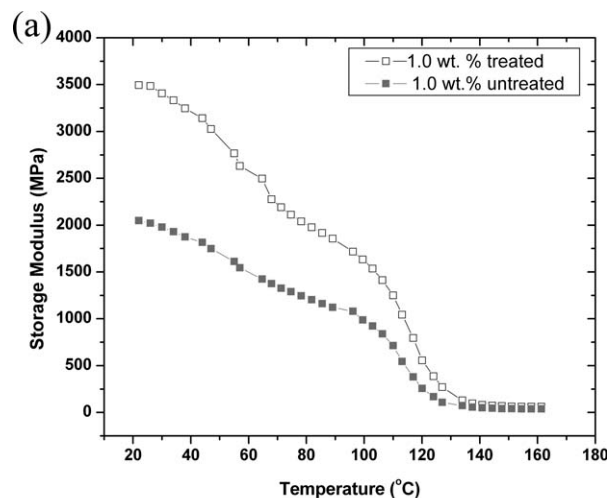


**Figure 6.** Comparison of the storage modulus ( $E'$ ) and loss modulus ( $E''$ ) of treated and untreated DP in epoxy matrix with DP concentration 1.0 wt %.

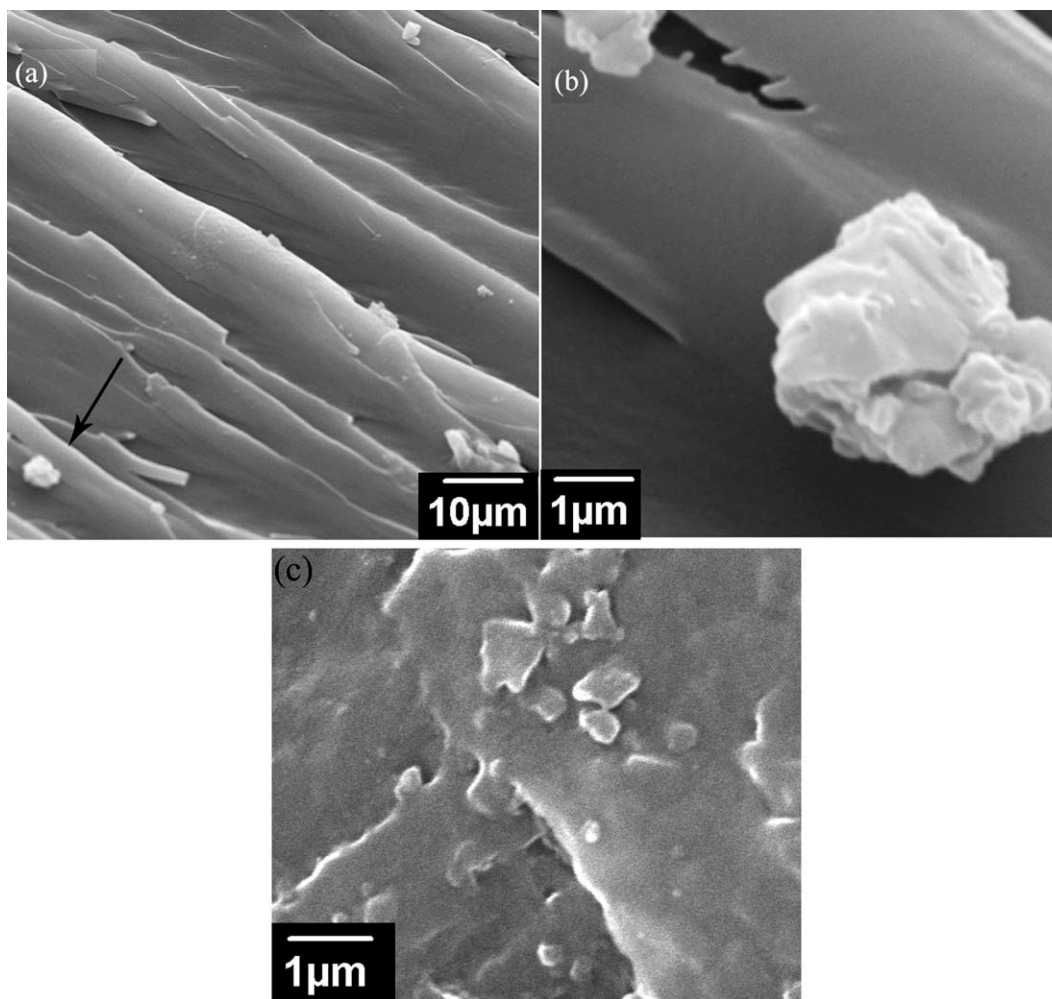


**Figure 7.** SEM images of diamond incorporated composites with epoxy matrix: (a) cross sectional view of 0.4 wt % sample, (b) high magnification image of the area indicated by arrow in (a) part, (c) plane view of 1.0 wt % sample.

Homogeneous dispersion makes more DP surfaces available for interaction with the surrounding epoxy matrix. Load can be transferred from matrix to filler either through chemical bonding, or van der Waals or electrostatic interaction or micromechanical interlocking between matrix and filler. Due to carboxylic groups attached to diamond particle surface, as a result of acid treatment, electrostatic type of interaction exist among diamond particles and epoxy rings. This is through the lone pair electrons present in the epoxy ring ( $\triangle$ ) and at the diamond particle surface ( $\text{D}-\overset{\text{O}}{\parallel}{\text{C}}-\text{OH}$ ) due to carboxylic acid group attached with the surface of the particles. For higher concentration (i.e. 1.0 wt. %) of DP in epoxy matrix, storage modulus decreases to value 3529 MPa. High content of DP might lead to poor dispersion due to the formation of particles agglomeration which results in low interfacial stress with the epoxy, reduces the thermo-mechanical properties of composites. This can be observed from the SEM image of 1.0 wt.% loaded sample in Figure 7(c). In the image, aggregates and clusters of particles can be seen in the matrix. With increasing concentration, the surface/volume ratio of diamond aggregates decreases which in turn negatively affect the interfacial bonding between DP and

epoxy matrix. Agglomerated particles have poor adhesion to the matrix in comparison to well isolated particles; therefore, stress transfer is not properly achieved. Whereas on the other hand, hard and stiff nature of the diamond particles reduces the epoxy molecules mobility, resulting in increased value of hardness.

## CONCLUSIONS

The mechanical behavior of diamond-epoxy composites loaded with diamond particles up to 1.0 wt % was studied. The presented results showed that the incorporation of diamond particles up to 0.7 wt % markedly improves the reinforcement action given by the storage modulus and glass transition temperature. Higher content of DP ( $\geq 1$  wt %) resulted in agglomeration of DP which reduces the mechanical properties of diamond-epoxy composites. On the other hand, the hardness keeps on increasing with the increase of the content of DP.

## ACKNOWLEDGMENTS

The authors acknowledge the cooperation of Dr. Yu Guojun for providing diamond powder. The cooperation of Mr. Adnan saeed (from Gomal University) for hardness tests is gratefully

acknowledged. The authors acknowledge the cooperation of director Mr. M. Arif and other EPL members for technical support. Centre of Excellence for Science and Advanced Technology, Islamabad, Pakistan

## REFERENCES

- Monteiro, S. N.; de Deus, J. F.; d'Almeida, J. R. M. Proc. of SAMCONAMET Binational Congress, 2005, Sociedad Argentina de Materiales, Mar del Plata, Argentina, **2005**, p 1.
- Shenderova, O.; McGuire, G. Nanocrystalline Diamond. Nanomaterials Handbook; CRC Press: Boca Raton, FL, **2006** 203.
- Yu, S. J.; Kang, M. W.; Chang, H. C.; Chen, K. M.; Yu, Y. C. *J. Am. Chem. Soc.* **2005**, *127*, 17604.
- Khil, M. S.; Cha, D. I.; Kim, H. Y.; Bhattarai, N. J. *Biomed. Mater. Res. B* **2003**, *67*, 675.
- Liu, K. K.; Chen, M. F.; Chen, P. Y.; Lee, T. J. F.; Cheng, C. L.; Chang, C. C. *Nanotechnology* **2008**, *19*, 205102.
- Huang, H.; Pierstorff, E.; Osawa, E. *Nano. Lett.* **2007**, *7*, 3305.
- Huang, H.; Pierstorff, E.; Osawa, E. *ACS Nano*. **2008**, *2*, 203.
- Osswald, S.; Yushin, G.; Mochalin, V.; Kucheyev, S.; Gogotsi, Y. *J. Am. Chem. Soc.* **2006**, *128*, 11635.
- Mochalin, V.; Osswald, S.; Gogotsi, Y. *Chem. Mater.* **2009**, *21*, 273.
- Krueger, A.; Ozawa, M.; Jarre, G.; Liang, Y.; Stegk, J. *Phys. Stat. Sol.* **2007**, *204*, 2881.
- Osswald, S.; Mochalin, V.; Havel, M.; Yushin, G.; Gogotsi, Y. *Phys. Rev. B* **2009**, *80*, 075419.
- Osswald, S.; Mochalin, V.; Havel, M.; Yushin, G.; Gogotsi, Y. *Diamond Relat. Mater.* **2008**, *17*, 1122.
- Zhang, Q.; Mochalin, V.; Neitzel, I.; Knoke, I.; Han, J.; Klug, C. *Biomaterials* **2011**, *32*, 87.
- Dolmatov, V. J. *Superhard. Mater.* **2007**, *29*, 65.
- Monteiro, S. N.; Ruben, S. J.; Rodriguez, S. G.; Skury, A. L. *D. Diamond Relat. Mater.* **2007**, *16*, 974.
- Spitalsky, Z.; Kromka, A.; Matejka, L.; Cernoch, P.; Kovarova, J.; *Adv. Compos. Lett.* **2008**, *17*, 29.
- Ayatollahi, M. R.; Alishahi, E.; Shadlou, S. *Int. J. Fract* **2011**, *170*, 95.
- Zhai, Y. J.; Wang, Z. C.; Huang, W.; Huang, J. J.; Wang, Y. Y.; Zhao, Y. Q.; *Mater. Sci. Eng. A* **2011**, *528*, 7295.
- Neitzel, I.; Mochalin, V.; Knoke, I.; Palmese, G. R.; Gogotsi, Y.; *Composites Sci and Tech* **2011**, *71*, 710.
- Mochalin, V. N.; Neitzel, I.; Etzold, B. J. M.; Peterson, A.; Palmese, G.; Gogotsi, Y. *ACS Nano* **2011**, *5*, 7494.
- Lee, G. Y.; Dharan, C. K. H.; Ritchie, R. O. *Wear* **2002**, *252*, 322.
- Behler, K. D.; Stravato, A.; Mochalin, V.; Korneva, G.; Yushin, G.; Gogotsi, Y. *ACS Nano*. **2009**, *3*, 363.
- Ushizawa, K.; Sato, Y.; Mitsumori, T.; Machinami, T.; Ueda, T. *Chem. Phys. Lett.* **2002**, *351*, 105.
- Palmese, G. R.; McCullough, R. L. *J. Appl. Polym. Sci.* **1992**, *46*, 1863.
- Kulakova, I. I. *Phys. Solid State* **2004**, *46*, 636.
- Ji, S. F.; Jiang, T. L.; Xu, K.; Li, S. B. *Appl. Surf. Sci.* **1998**, *133*, 231.
- Strawhecker, K. E.; Manias, E. *Chem. Mater.* **2000**, *12*, 2943.
- Lee, C.; Leigh, D. A.; Pritchard, R. G.; Schultz, D.; Teat, S. J.; Timco, G. A.; Winpenny, R. E. P. *Nature* **2009**, *458*, 314.
- Wan, C.; Zhang, Y. *Polym. Test.* **2004**, *23*, 299.
- Zhou, T. H.; Ruan, W. H.; Rong, M. Z.; Zhang, M. Q.; Mai, Y. L. *Adv. Mater.* **2007**, *19*, 2667.